UNSTEADY HEAT AND MASS TRANSFER DURING FROST FORMATION IN A FIN-AND-TUBE HEAT EXCHANGER

Kristian Lenić, Anica Trp, Bernard Franković
Faculty of Engineering University of Rijeka, Vukovarska 58, HR-51000 Rijeka, Croatia
Phone: + 385 51 651 518, Fax: + 385 51 675 801,
E-mail: kristian.lenic@riteh.hr, anica.trp@riteh.hr, bernard.frankovic@riteh.hr

Abstract: *In the paper, numerical and experimental analyses of heat and mass transfer during frost formation on a fin-and-tube heat exchanger have been performed. The modelling of frost formation on cold surfaces placed in a humid air stream requires a complex mathematical approach. Results have shown that frost layer growth is faster with higher inlet air humidity. Frost layer formation significantly influences the heat transfer between air and refrigerant. Using the developed mathematical model, the algorithm and the computer code, which have been experimentally validated, it is possible to predict a decrease of exchanged heat flux in the heat exchanger under frost growth conditions.*

Key words: frost layer formation, fin-and-tube heat exchanger, numerical analysis

1. INTRODUCTION

Frost layer grows on finned surfaces of a fin-and tube heat exchanger when fin surface temperature becomes smaller than the temperature of water freezing. The porous structure of frost layer consists of ice crystals and air gaps. Whereas frost layer contains air pores with low thermal conductivity, the whole frost layer represents significant thermal resistance. The thermal resistance of frost layer and reduction of air flow due to augmented pressure drop causes significant decreasing of heat exchanger efficiency. This has an effect on space cooling quality and working behaviour of the whole device. The principal aim of frost formation analysis is estimation of exchanged heat flux under transient conditions of augmented thermal resistance.

Frost formation process depends on water vapour transfer from air stream into frost layer, diffusion rate of water vapour into the frost layer and thermal conduction inside the layer. One part of the water vapour flux which transfers from the air stream has been deposited on the frost surface and increases the frost thickness. The other part of the water vapour flux enters the frost layer and thus increases its density. Accuracy of determination of water mass flux which enters the frost layer has a crucial influence on accuracy of determination of frost layer growth rate.

Many authors divide the whole frost formation process into three different periods: crystal growth period, frost growth period and fully developed frost formation period.

Porosity, i.e. volume fraction of air inside a segment of frost layer, defined as a ratio of air volume and total volume of the segment, can be expressed using air and ice densities:

$$\varepsilon = \frac{\rho_{\mathrm{i}} - \rho_{\mathrm{fl}}}{\rho_{\mathrm{i}} - \rho_{\mathrm{a}}} \tag{1}$$

Porosity can be any value between 0 and 1 ($0 \leq \varepsilon \leq 1$). For pure ice porosity amounts $\varepsilon = 0$.
Frost layer density can be expressed as:

$$\rho_{\mathrm{fl}} = \varepsilon \cdot \rho_{\mathrm{a}} + (1 - \varepsilon) \cdot \rho_{\mathrm{i}} \tag{2}$$

The majority of models developed so far can be classified into several groups. One is the group of models which predict the variations of frost properties from the diffusion equation applied to the frost layer and then calculate the amount of heat and mass transfer in the frost layer by using the correlations on the air-side. This approach is used by *K. S. Lee et al.* [1], *B. W. Jones et al.* [2] and *A. Z. Sahin* [3]. The second group of modelling method gives some improvements and analyzes the air flow with boundary layer equations and predicts the frost properties by using the correlations. *K. S. Lee et al.* [4] developed a mathematical model without using the correlations for air boundary layer zone and frost layer zone. *Le Gall et al.* [5] developed a transient one-dimensional model for frost growth and frost density changes formed on cooled surfaces in the humid air stream. *Lüer* and *Beer* [6] theoretically and experimentally investigated the frost formation process on parallel plates in a humid air stream in laminar flow. *Na* and *Weeb* [7,8] investigated basic phenomena related to frost layer formation and growth. They experimentally measured water vapour mass flux from air stream to frost layer. Through analysis of measured data, they stated that the partial pressure of water vapour on frost layer surface is greater than partial pressure of water vapour for the temperature of frost layer surface, i.e. that air near the surface of frost layer is supersaturated.

In all abovementioned models, a number of assumption have been used causing some divergence regarding real physical process. This indicates the necessity of further investigations in that field.

As a first improvement, a calculation of air velocity, temperature and humidity fields has been performed allowing a more exact description of heat and mass transfer. Furthermore, the problem has been solved as transient and two-dimensional. In the presented mathematical model, some of the latest results from previous models have been introduced including determination of air state at air-frost interface.

2. MATHEMATICAL MODEL

A domain of calculation has been extracted from the physical model and includes one half of space between fins, as presented in figure 1. The domain consists of two areas: subdomain of humid air and subdomain of frost layer which are delimited by air-frost interface. Lower boundary represents a cold fin surface and at the top boundary the symmetrical boundary condition has been presumed.

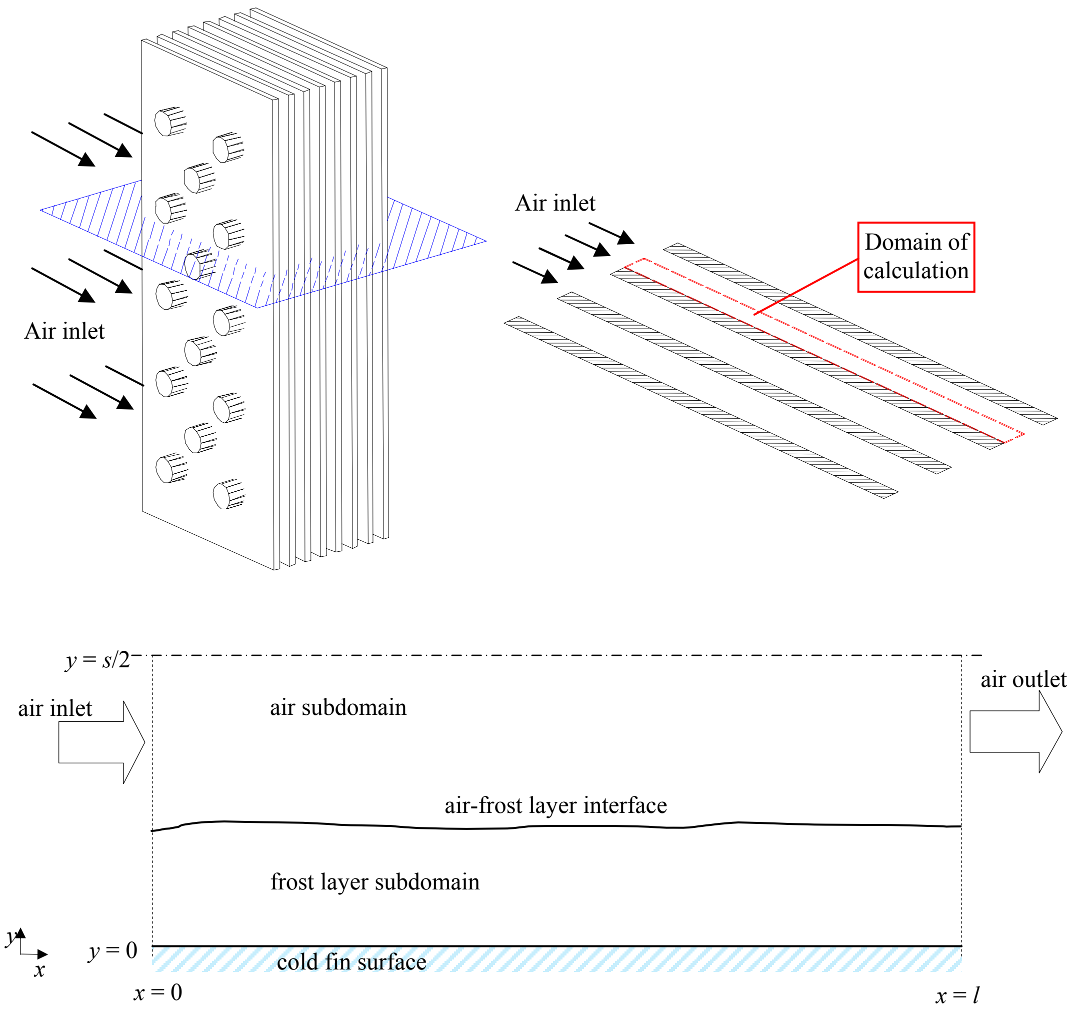

Figure 1. Analyzed fin-and-tube heat exchanger and domain of numerical calculation

2.1. Governing equations

In the air subdomain, physical phenomena of heat and mass flow have been described using continuity, momentum and energy equations as well as water vapour transport equation. For the frost layer subdomain, energy equation and modified diffusion equation have been used.

Air subdomain

$$\frac{\partial}{\partial x}\left(\rho_{\mathrm{a}}\, u_x\right)+\frac{\partial}{\partial y}\left(\rho_{\mathrm{a}}\, u_y\right)=0 \qquad (3)$$

$$\rho_{\mathrm{a}}\frac{\partial u_x}{\partial t}+\rho_{\mathrm{a}}\left(u_x\frac{\partial u_x}{\partial x}+u_y\frac{\partial u_x}{\partial y}\right)=-\frac{\partial p}{\partial x}+\eta\left(\frac{\partial^2 u_x}{\partial x^2}+\frac{\partial^2 u_x}{\partial y^2}\right) \qquad (4)$$

$$\rho_{\mathrm{a}}\frac{\partial u_y}{\partial t}+\rho_{\mathrm{a}}\left(u_x\frac{\partial u_y}{\partial x}+u_y\frac{\partial u_y}{\partial y}\right)=-\frac{\partial p}{\partial y}+\eta\left(\frac{\partial^2 u_y}{\partial x^2}+\frac{\partial^2 u_y}{\partial y^2}\right) \qquad (5)$$

$$\rho_{\mathrm{a}}\frac{\partial \vartheta_{\mathrm{a}}}{\partial t}+\rho_{\mathrm{a}}\cdot\left(u_x\frac{\partial \vartheta_{\mathrm{a}}}{\partial x}+u_y\frac{\partial \vartheta_{\mathrm{a}}}{\partial y}\right)=\frac{\lambda_{\mathrm{a}}}{c_{\mathrm{p,a}}}\left(\frac{\partial^2 \vartheta_{\mathrm{a}}}{\partial x^2}+\frac{\partial^2 \vartheta_{\mathrm{a}}}{\partial y^2}\right) \tag{6}$$

$$\rho_{\mathrm{a}}\frac{\partial w}{\partial t}+\rho_{\mathrm{a}}\cdot\left(u_x\frac{\partial w}{\partial x}+u_y\frac{\partial w}{\partial y}\right)=\rho_{\mathrm{a}}\cdot D\cdot\left(\frac{\partial^2 w}{\partial x^2}+\frac{\partial^2 w}{\partial y^2}\right) \tag{7}$$

Frost layer subdomain

$$\rho_{\mathrm{fl}}\frac{\partial \vartheta_{\mathrm{fl}}}{\partial t}=\frac{\partial}{\partial x}\left(\frac{\lambda_{\mathrm{fl}}}{c_{\mathrm{p,fl}}}\frac{\partial \vartheta_{\mathrm{fl}}}{\partial x}\right)+\frac{\partial}{\partial y}\left(\frac{\lambda_{\mathrm{fl}}}{c_{\mathrm{p,fl}}}\frac{\partial \vartheta_{\mathrm{fl}}}{\partial y}\right)+q_{\mathrm{sub}}\frac{\partial \rho_{\mathrm{ls}}}{\partial t} \tag{8}$$

$$\frac{\partial \rho_{\mathrm{fl}}}{\partial t}=\frac{\partial}{\partial x}\left(D_{\mathrm{eff}}\rho_{\mathrm{a}}\frac{\partial(\rho_{\mathrm{v}}/\rho_{\mathrm{a}})}{\partial x}\right)+\frac{\partial}{\partial y}\left(D_{\mathrm{eff}}\rho_{\mathrm{a}}\frac{\partial(\rho_{\mathrm{v}}/\rho_{\mathrm{a}})}{\partial y}\right) \tag{9}$$

2.2. Initial conditions

Air subdomain

Initial distributions of air temperatures and humidities are uniform and initial velocity is equal to zero.

$$\vartheta_{\mathrm{z}0}=\vartheta_{\mathrm{in}},\ w_0=w_{\mathrm{in}},\ u_{x0}=0,\ u_{y0}=0$$

Frost layer subdomain

It is assumed that the initial temperature of frost layer is equal to cold surface temperature. This assumption is valid if initial thickness is adequately small so that thermal resistance of the frost layer can be neglected when compared to air side thermal resistance.

$$\vartheta_{\mathrm{fl}0}=\vartheta_{\mathrm{s}}$$

For the computation of frost layer growth, it is required to provide frost layer thickness and density at an early stage of frost formation. *Jones* and *Parker* [2] investigated the influence of different initial frost layer thickness on calculation results. In accordance with their results the initial frost layer thickness is assumed to be 0.02 mm. Authors also evaluated the effect of the initial value of the frost density on the frost growth rate by changing the value from 8 to 48 kg/m^3. They found that the frost density and thickness converged to the same value. Based on their investigation, in this work the initial value of frost density have been assumed as follows:

$$\rho_{\mathrm{fl}\ 0}=30\ \mathrm{kg/m^3}$$

2.3. Boundary conditions

Left (inlet) boundary $x = 0$, $0<y< s/2$

Air subdomain $u_x=u_{\mathrm{in}},\ u_y=0,\ \vartheta_{\mathrm{z}}=\vartheta_{\mathrm{in}},\ w=w_{\mathrm{in}}$

Frost layer subdomain $\frac{\partial \vartheta_{\mathrm{fl}}}{\partial x}=0$, $\frac{\partial(\rho_{\mathrm{v}}/\rho_{\mathrm{a}})}{\partial x}=0$

Top boundary – symmetry plane $y = s/2$, $0<x< l$

$$u_y=0\,,\ \frac{\partial u_x}{\partial y}=0\,,\ \frac{\partial \vartheta_{\mathrm{a}}}{\partial y}=0\,,\ \frac{\partial w}{\partial y}=0$$

Right (outlet) boundary $x = l$, $0<y< s/2$

Air subdomain $\frac{\partial u_x}{\partial x}=0$, $\frac{\partial u_y}{\partial x}=0$, $\frac{\partial \vartheta_{\mathrm{z}}}{\partial x}=0$, $\frac{\partial w}{\partial x}=0$

Frost layer subdomain $\frac{\partial \vartheta_{\mathrm{fl}}}{\partial x}=0$, $\frac{\partial(\rho_{\mathrm{v}}/\rho_{a})}{\partial x}=0$

Bottom boundary $y = 0$, $0<x< l$

$$\vartheta_{\mathrm{fl}}=\vartheta_{\mathrm{s}}\,,\ \frac{\rho_{\mathrm{v}}}{\rho_{\mathrm{a}}}=\frac{\rho_{\mathrm{v}}(\vartheta_{\mathrm{s}})}{\rho_{\mathrm{a}}(\vartheta_{\mathrm{s}})}$$

Air-frost layer interface

Air velocity $u_x=0$, $u_y=0$

Air humidity

In their recent investigations, *Na* and *Weeb* [7,8] assumed that the partial pressure of water vapour on a frost layer surface is greater than the partial pressure of water vapour for the temperature of a frost layer surface, i.e. that air near the surface of frost layer is supersaturated. Referential value for defining the supersaturation state is supersaturation degree defined as follows:

$$S=\frac{p_{\mathrm{v}}-p_{\mathrm{v,\,sat}}}{p_{\mathrm{v,\,sat}}} \tag{10}$$

Using the above definition, mass fraction of water vapour in air on air-frost interface is:

$$w_{\mathrm{fs}}=0{,}622\cdot\frac{(1+S)p_{\mathrm{v,\,sat}}}{p-(1+S_{\mathrm{v}})p_{\mathrm{v,\,sat}}} \tag{11}$$

Supersaturation degree is calculated using the following equation:

$$S=0{,}808\left(\frac{p_{\mathrm{v},\infty}}{p_{\mathrm{v,sat},\infty}}\right)\left(\frac{p_{\mathrm{v,\,sat,fs}}}{p_{\mathrm{v,sat},\infty}}\right)^{-0{,}657}-1 \tag{12}$$

Temperature

Temperature of frost layer surface is calculated using the following boundary condition for the energy equation:

$$\lambda_{\mathrm{a}} \frac{\partial \vartheta_{\mathrm{a}}}{\partial y} = \lambda_{\mathrm{fl}} \frac{\partial \vartheta_{\mathrm{fl}}}{\partial y} + q_{\mathrm{sub}} \rho_{\mathrm{fl}} \frac{\mathrm{d} y_{\mathrm{fl}}}{\mathrm{d} t} \tag{13}$$

Density of new frost created at a frost surface
It is assumed that the density of new frost is equal to frost density at the surface

$$\left(\frac{\partial \rho_{\mathrm{fl}}}{\partial y} \right)_{\mathrm{fs}} = 0$$

Velocity of frost surface moving
One part of water vapour mass flux which transfers from the air stream has been deposited on the frost surface and increases the frost thickness. The other part of water vapour flux enters the frost layer and increases its density, figure 2.

$$\dot{m}_{\mathrm{a}} = \dot{m}_{\Delta y} + \dot{m}_{\mathrm{diff}} \tag{14}$$

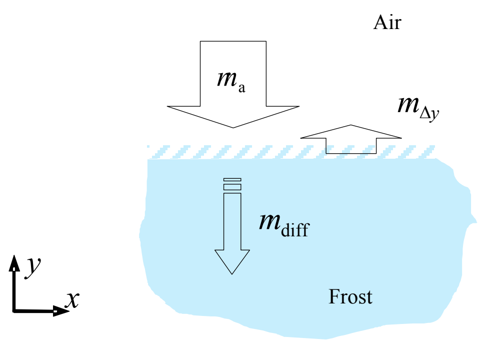

Figure 2. Water vapour mass fluxes on frost layer surface

Frost layer growth rate has been calculated using total water vapour mass flux and diffusive mass flux on a frost layer surface. Mass flux density of water vapour transferring from air to a frost layer surface is proportional to the gradient of air humidity:

$$\dot{m}_{\mathrm{a}} = \rho_{\mathrm{a}} \cdot D \cdot \frac{\mathrm{d} w}{\mathrm{d} y} \tag{15}$$

Mass flux density which increases the frost layer density absorbed by the frost layer is given by:

$$\dot{m}_{\mathrm{diff}} = -\rho_{\mathrm{a}} \cdot D_{\mathrm{eff}} \cdot \frac{\mathrm{d}\left(\rho_{\mathrm{v}} / \rho_{\mathrm{a}}\right)}{\mathrm{d} y} \tag{16}$$

Mass flux density responsible for layer thickness growth is:

$$\dot{m}_{\Delta \mathrm{y}} = \rho_{\mathrm{fl}} \frac{\mathrm{d} y_{\mathrm{fl}}}{\mathrm{d} t} = \dot{m}_{\mathrm{a}} - \dot{m}_{\mathrm{diff}} \tag{17}$$

The frost layer growth rate is thus:

$$\frac{\mathrm{d}y_{\mathrm{ls}}}{\mathrm{d}t} = \frac{1}{\rho_{\mathrm{ls}}}\dot{m}_{\Delta \mathrm{y}} = \frac{1}{\rho_{\mathrm{ls}}}\left(\dot{m}_{\mathrm{z}} - \dot{m}_{\mathrm{dif}}\right) \tag{18}$$

Physical properties of frost layer
The effective thermal conductivity of the frost layer is related to the frost density. In this study, the following correlation proposed by *Lee et al.* [4] is used:

$$\lambda_{\mathrm{fl}} = 0{,}132 + 3{,}13 \cdot 10^{-4} \rho_{\mathrm{fl}} + 1{,}6 \cdot 10^{-7} \rho_{\mathrm{fl}}^{\ 2} \tag{19}$$

The specific heat of the frost layer is obtained from the densities and specific heats of ice and humid air as well as density and porosity of the frost layer using:

$$c_{\mathrm{p,\,fl}} = \frac{1}{\rho_{\mathrm{fl}}}\left[\rho_{\mathrm{i}}(1-\varepsilon)c_{\mathrm{p,\,i}} + \rho_{\mathrm{a}}\varepsilon\, c_{\mathrm{p,a}}\right] \tag{21}$$

The effective diffusion coefficient, as proposed by *Na* and *Weeb* [7,8], has been calculated using:

$$D_{\mathrm{eff}} = D \cdot \varepsilon \cdot \tau = D \cdot \varepsilon \cdot \frac{1+\varepsilon}{2} \tag{22}$$

Where tortuosity factor is defined as follows:

$$\tau = \frac{1+\varepsilon}{2} \tag{23}$$

3. NUMERICAL SOLUTION

The governing equations are discretised using control volume method. Staggered grids for velocity components have been used to avoid physically unrealistic pressure field in the air subdomain. The convection-diffusion terms have been discretised using power-law scheme and the resulting set of linearised discretisation equations have been solved using an iterative procedure. A fully implicit method has been used for time-stepping treatment. For the velocity-pressure coupling the SIMPLER algorithm has been applied [8]. Physical property data have been stored in a separate input files. Algorithm has been implemented in a self-written FORTRAN code and solved on a personal computer (2,6 GHz).

4. EXPERIMENTAL VALIDATION

The validation of the numerical model and developed computer code has been analysed by comparison between numerical and experimental data. Inlet conditions during the experimental investigation have been used as input data in numerical simulations. An experimental line consisted of an aluminium cooled plate placed in a humid air stream with controlled inlet conditions. Figures 3 and 4 shows time-wise frost layer thickness variations for two different inlet conditions with comparison of numerical and experimental data.

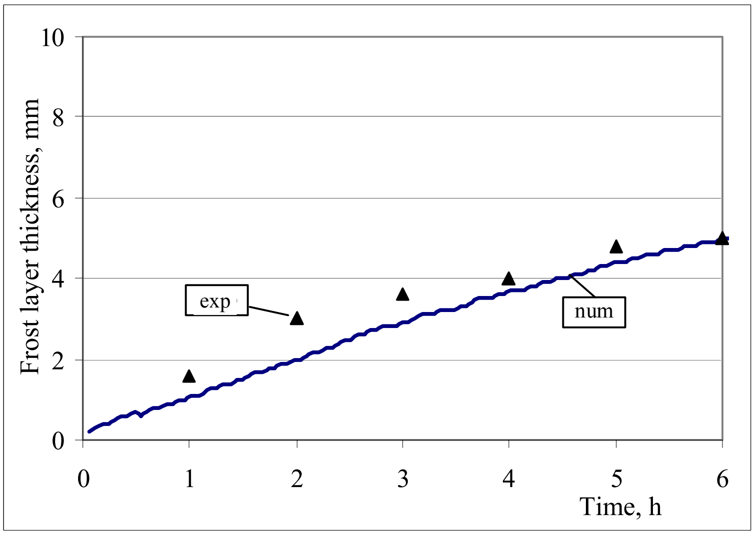

Figure 3. Time-wise frost layer thickness variations – comparison of experimental and numerical values ($\vartheta_{a,in}$ = 21.4 °C, w_{in} = 0.0062 kg/kg, $u_{x,in}$= 0.6 m/s, ϑ_{fs} = -19.5 °C)

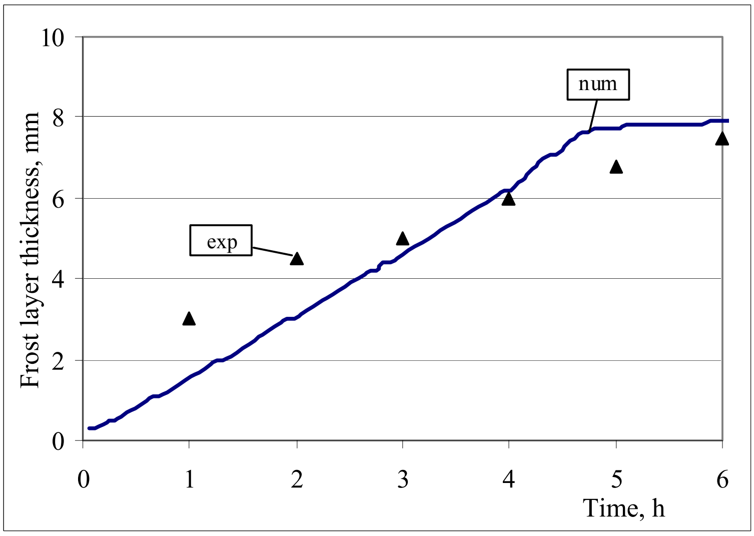

Figure 4. Time-wise frost layer thickness variations – comparison of experimental and numerical values ($\vartheta_{a,in}$ = 19.8 °C, w_{in} = 0.0085 kg/kg, $u_{x,in}$= 0.6 m/s, ϑ_{fs} = -20.5 °C)

The comparison between numerical predictions and experimental data for frost layer growth in a humid air stream shows compatibility regarding trends of analysed variables. The results obtained indicated that a developed numerical procedure could be efficiently used to simulate the physical process of frost layer formation.

5. RESULTS AND DISCUSSION

After the validation of the mathematical model and computer code, the numerical analysis were performed for a fin-and-tube heat exchanger with the following geometrical characteristics: fin thickness 0.001 m, space between fins 0.006 m, fins width 0.048 m, total number of pipes 189, total number of fins 210, heat exchanger surface 18 m^2, longitudinal pipe distance 0.016 m, transversal pipe distance 0.014 m, outer pipe diameter 0.01 m and inside pipe diameter 0.008 m.

A set of numerical calculations has been performed in order to evaluate the influence of inlet air velocity, temperature and humidity on the frost growth rate. A numerical analysis has been carried out for different inlet air velocities, temperatures and humidities. Longitudinal distributions of frost layer thickness for different periods of frost formation and different inlet humidities are shown on figures 5 and 6. Velocity vector fields for different periods of frost formation and different inlet humidities are shown on figures 7 and 8.

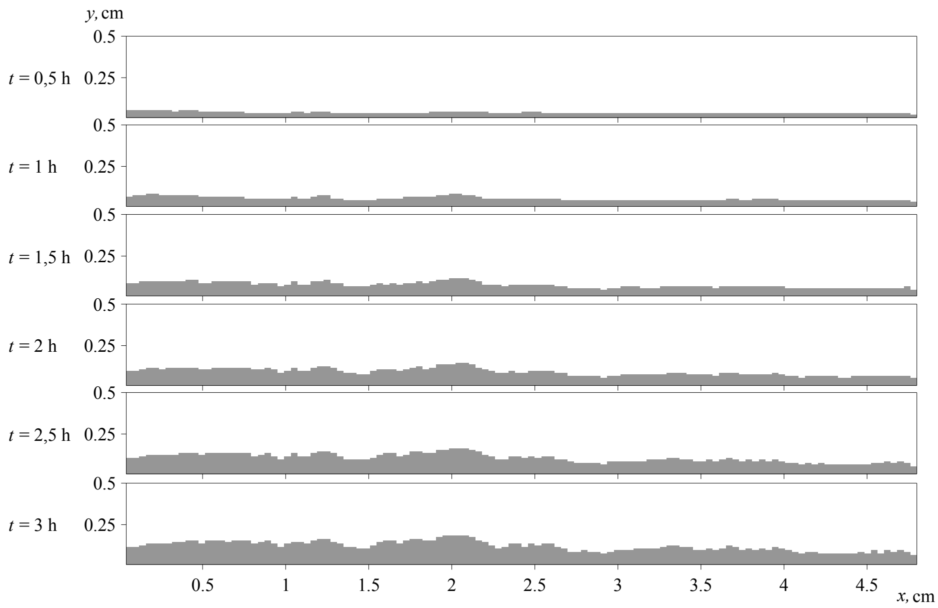

Figure 5. Longitudinal distributions of frost layer thickness for different periods of frost formation ($\vartheta_{a,in}$ = 12 °C, w_{in} = 0.002 kg/kg, $u_{x,in}$= 1 m/s, ϑ_{fs} = -12 °C)

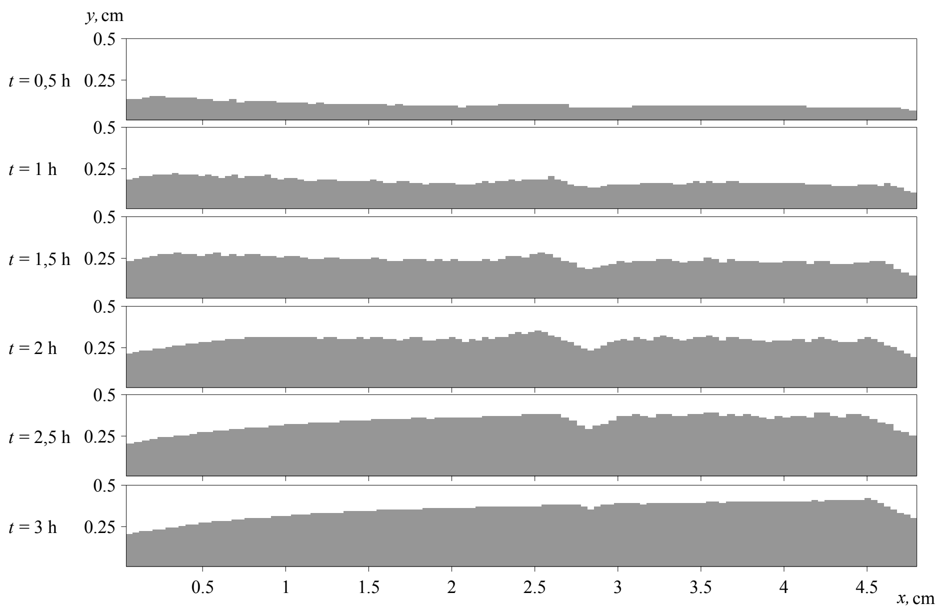

Figure 6. Longitudinal distributions of frost layer thickness for different periods of frost formation ($\vartheta_{a,in}$ = 12 °C, w_{in} = 0.006 kg/kg, $u_{x,in}$= 1 m/s, ϑ_{fs} = -12 °C)

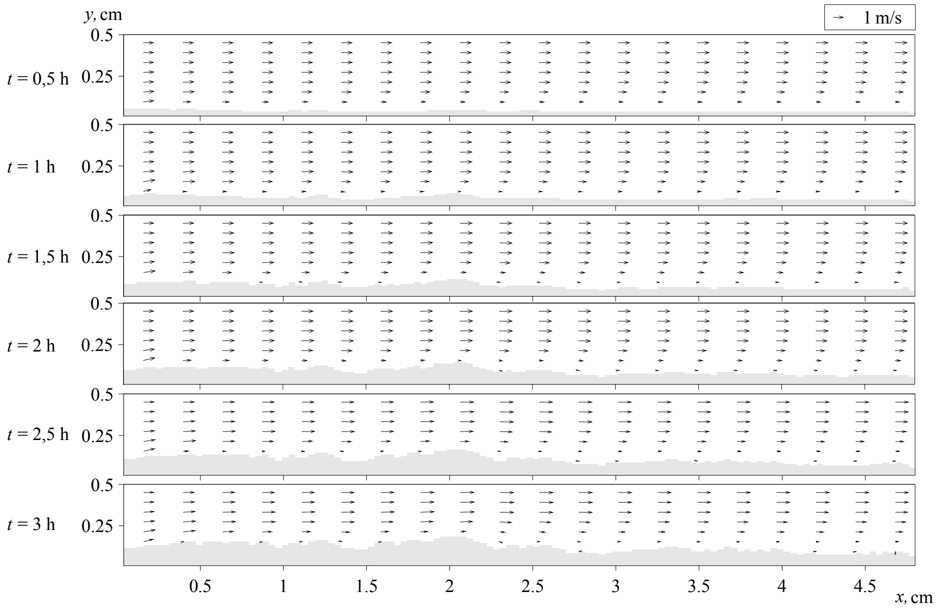

Figure 7. Velocity vector fields for different periods of frost formation ($\vartheta_{a,in}$ = 12 °C, w_{in} = 0.002 kg/kg, $u_{x,in}$= 1 m/s, ϑ_{fs} = -12 °C)

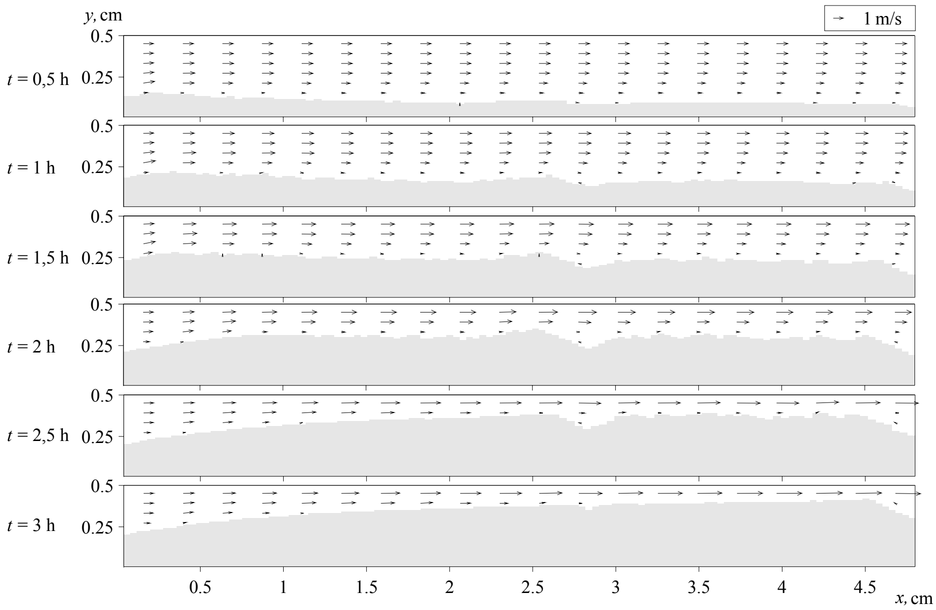

Figure 8. Velocity vector fields for different periods of frost formation ($\vartheta_{a,in}$ = 12 °C, w_{in} = 0.006 kg/kg, $u_{x,in}$= 1 m/s, ϑ_{fs} = -12 °C)

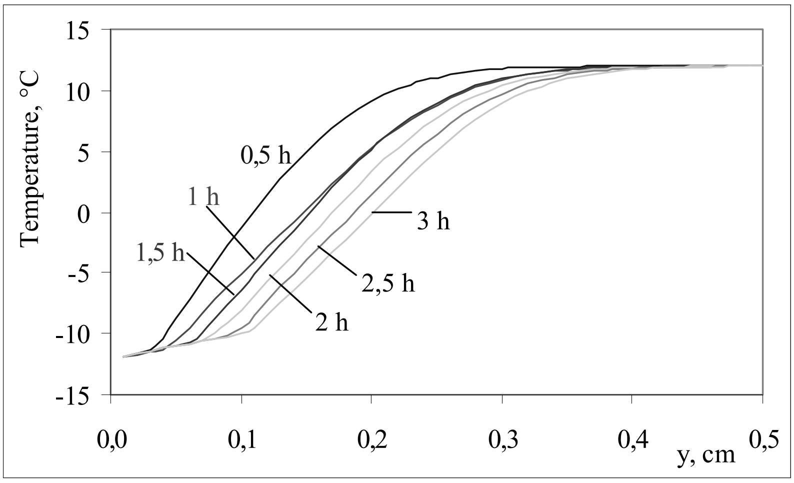

Figure 9. Transversal distributions of temperatures for different periods of frost formation x = 15 mm ($\vartheta_{a,in}$ = 12 °C, w_{in} = 0.002 kg/kg, $u_{x,in}$= 1 m/s, ϑ_{fs} = -12 °C)

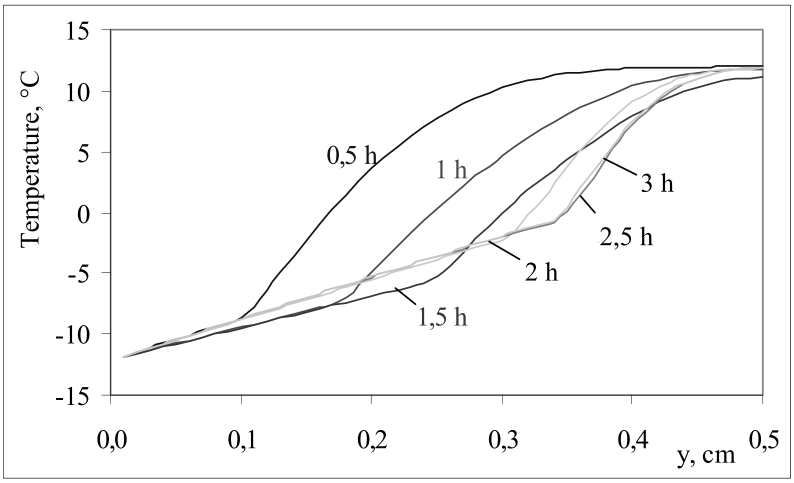

Figure 10. Transversal distributions of temperatures for different periods of frost formation x = 15 mm ($\vartheta_{a,in}$ = 12 °C, w_{in} = 0.006 kg/kg, $u_{x,in}$= 1 m/s, ϑ_{fs} = -12 °C)

Due to the heat transfer from air to frost layer, cooling of air stream near frost surface occurs. Distribution of temperature field is stratified because the laminar flow has been assumed. The average temperature at transversal cross-section becomes lower from inlet to outlet. During regular operation the frost layer becomes thicker and frost surface temperature becomes higher due to increased thermal resistance.

In the case with higher inlet air humidity (w_{in} = 0.006 kg/kg) frost growth is more intensive compared to case with lower inlet air humidity (w_{in} = 0.006 kg/kg). In the beginning, the frost growth is more intensive at the inlet part of heat exchanger and along whole domain, first and second phases of frost formation occur i.e. crystal growth phase and frost growth phase. As frost layer grows, because of increased thermal resistance, the temperature of frost layer surface becomes higher. When the frost surface temperature reaches 0°C, the third phase of frost growth formation takes place. This first occurs at inlet boundary zone. Then "the third phase zone" spreads to outlet boundary. In this case both the second and the third phase of frost formation are present.

Frost layer growth is more intensive under the higher air humidity because of the higher gradient of air humidity near the frost surface in the boundary layer. This influence of air humidity on frost layer growth rate is significant.

6. CONCLUSIONS

Investigations described in this paper have included numerical and experimental analyses of heat and mass transfer during frost formation on a fin-and-tube heat exchanger. Results have shown that phenomena of frost formation on a cold surfaces placed in a humid air stream requires a complex mathematical approach. During the frost layer growth, an increase of frost density occurs. The numerical analysis should take into account the porous nature of the frost layer and appropriate physical properties must be calculated.

It can be concluded that the frost layer growth is faster when the inlet air humidity is higher. Frost layer formation significantly influences the heat transfer from air to refrigerant which evaporates inside the heat exchanger pipes. Using a developed mathematical model, algorithm and computer code, which have been experimentally validated, it is possible to predict the frost growth rate and thus a decrease of exchanged heat flux in heat exchanger under the frost growth conditions.

7. LIST OF SYMBOLS

c	specific heat (J kg^{-1} K^{-1})
D	diffusivity (m^2 s^{-1})
l	domain length (m)
$\dot{m}_z$	water vapour mass flux (kg m^{-2} s^{-1}),
p	pressure (Pa)
q	specific heat of sublimation (J kg^{-1})
S	supersaturation degree
s	distance between fins (m)
t	time (s)
u_x	x-velocity component (m s^{-1})
u_y	y-velocity component (m s^{-1})
w	mass fraction of water vapour in air (kg kg^{-1})
x	coordinate (m)
y	coordinate (m)
ε	porosity
η	dynamic viscosity (kg s^{-1} m^{-1}) efficiency
ϑ	temperature (ºC)
λ	thermal conductivity (W m^{-1} K^{-1})
ρ	density (kg m^{-3})
τ	tortuosity factor

Indexes

a	air
diff	related to diffusion into frost layer
eff	effective
fl	frost layer
fs	frost surface
i	ice
s	fin surface
in	inlet
sat	saturated
v	water vapour
Δy	related to layer thickness increasing
0	initial value

REFERENCES

[1] Lee, K. S., Kim, W. S., Lee, T. H.: *A one-dimensional model for frost formation on a cold surface*, International Journal of Heat and Mass Transfer, 40 (1997), 4359-4365

[2] Jones, B. W., Parker, J. D.: *Frost formation with varying environmental parameters,* Journal of Heat Transfer, 97 (1975), 255-259

[3] Sahin, A. Z.: *An analytical study of frost nucleation and growth during the crystal growth period,* International Journal of Heat and Mass Transfer, 30 (1995), 321-330

[4] Lee, K., Jhee, S., Yang, D.: *Prediction of the frost formation on a cold flat surface*, International Journal of Heat and Mass Transfer, 46 (2003), 3789-3796

[5] Le Gall, R., Grillot, J. M., Jallut, C.: *Modelling of frost growth and densification,* International Journal of Heat and Mass Transfer, 40 (1997), 3177-3187

[6] Lüer, A., Beer, H.: *Frost deposition in a parallel plate channel under laminar flow conditions,* International Journal of Thermal Science, 39 (2000), 85-95

[7] Na, B., Weeb, R. L.: *New model for frost growth rate*, International Journal of Heat and Mass Transfer, 47 (2004), 925-936

[8] Na, B., Weeb, R. L.: *Mass transfer on and within a frost layer*, International Journal of Heat and Mass Transfer, 47 (2004), 899-911

[9] Patankar, S. V.: *Numerical Heat Transfer and Fluid Flow*, Hemisphere Publishing Corporation, Taylor & Francis Group, New, York, 1980

[10] Tao, Y. X., Besant, R. W., Reykallah, K. S.: *A mathematical model for predicting the densification and growth of frost on a flat plate,* International Journal of Heat and Mass Transfer, 36 (1993), 353-363

[11] Hayarishi, Y., Aoki, A., Adachi, S., Hori, K.: *Study of frost properties correlating with frost formation types*, Journal of Heat Transfer, 99 (1977), 239-245

[12] Sanders, C. T.: *The influence of frost formation and defrosting on the performance of air coolers*, Ph.D. thesis, Delft Technical University, Delft, 1974

[13] Bošnjaković, F.: *Nauka o toplini II*, Tehnička knjiga, Zagreb, 1976 (in Croatian)

[14] Lenić, K.: *Analysis of heat and mass transfer during frost formation on fin-and-tube heat exchangers*, D.Sc. thesis, Faculty of Engineering University of Rijeka, Rijeka, Croatia, 2006 (in Croatian)

NESTACIONARNA IZMJENA TOPLINE I TVARI PRI STVARANJU LEDA U LAMELNOM IZMJENJIVAČU TOPLINE

Sažetak: *U radu je provedena numerička i eksperimentalna analiza izmjene topline i tvari tijekom nastanka ledenog sloja na lamelnom izmjenjivaču topline. Modeliranje stvaranja ledenog sloja na hladnim površinama podvrgnutim strujanju vlažnoga zraka zahtijeva složeni matematički pristup. Rezultati su pokazali da je brzina rasta ledenog sloja veća pri većim ulaznim vlažnostima zraka. Nastanak ledenog sloja značajno utječe na izmjenu topline između zraka i radne tvari. Koristeći razvijeni matematički model, algoritam i eksperimentalno potvrđeni računalni program moguće je predvidjeti smanjenje izmijenjenog toplinskog toka u izmjenjivaču topline pri različitim uvjetima nastanka ledenog sloja.*

Ključne riječi: nastanak ledenog sloja, lamelni izmjenjivač topline, numerička analiza